Iris the Picture of Health: Towards Medical Diagnosis of Diseases based on Iris Pattern

Conference Paper · October 2015

DOI: 10.1109/ICDIM.2015.7381861

3 authors:

Sare Amerifar
Tarbiat Modares University
2 PUBLICATIONS **17** CITATIONS
SEE PROFILE

Alireza Tavakoli Targhi
Shahid Beheshti University
34 PUBLICATIONS **224** CITATIONS
SEE PROFILE

Mohammad Mahdi Dehshibi
Universitat Oberta de Catalunya
53 PUBLICATIONS **378** CITATIONS
SEE PROFILE

Iris the Picture of Health: Towards Medical Diagnosis of Diseases based on Iris Pattern

Sare Amerifar
ISPR Lab., Department of Computer Science
Faculty of Mathematics, Shahid Behshti University
Tehran, Iran
s.amerifar@isprlab.com

Alireza Tavakoli Targhi
ISPR Lab., Department of Computer Science
Faculty of Mathematics, Shahid Behshti University
Tehran, Iran
a_tavakoli@sbu.ac.ir

Mohammad Mahdi Dehshibi
ISPR Lab., Department of Computer Science
Faculty of Mathematics, Shahid Behshti University
Tehran, Iran
dehshibi@iranprc.org

***Abstract*—Complementary medicine emphasizes therapies which are claimed to improve quality of life, prevent disease, and address conditions that conventional medicine has limited success in curing. Iridology is an alternative medicine technique which examines patterns, colors, and other characteristics of the iris to determine information about a patient's systemic health. The objective of this paper is to validate the use of iridology to find out body's organs abnormalities. The proposed method consists of (i) finding the center of iris and its radius, (ii) mapping iridology chart into extracted iris image, and (iii) geometrical analyzing characteristics of the iris to find out which abnormities may be exist in the patient. Two sets of experiment were conducted which in the first one, performance of the proposed was evaluated on CASIA Iris Image Database; and in the second set, a subjective test was given from an iridologist. It was observed in the course of experiments that the accuracy of the proposed method is comparable with that of given from the iridologist. The results of a case study is demonstrated in this paper which shows a 82% correct classification for subjects who are suffered from kidney problems and 93% correct classification for normal subjects. However, it is necessary to perform extensive studies with diseases that do not have ocular manifestations according to conventional medicine in order to validate iridology as a valid scientific technique.**

Keywords*— Iridology; Pervasive Healthcare; Image Processing; Gradient Vector Flow.

I. INTRODUCTION

Traditional image processing aims at solving fundamental problems dealing with them; however, nowadays, image processing techniques in conjunction with machine learning methods are used to solving real world problems which can be considered as a solution for interdisciplinary problems. Artifacts such as age detection [1], surveillance [2], traffic management [3], and medical image analysis [4] are among the most promising applications of this discipline.

Complementary medicine is those therapies that are claimed to improve quality of life, prevent disease, and address conditions that conventional medicine has had limited success in curing, such as chronic back pain and certain cancers. Proponents of complementary medicine believe that these approaches to healing are safer and more natural and have been shown through experience to work. In certain countries, complementary medical practices are widely used methods of health care. However, many practitioners of modern conventional medicine believe these practices are unorthodox and unproven.

Iridology is a form of complementary medicine whose proponents believe patterns, colors, and other characteristics of the iris can be examined to determine information about a patient's systemic health. Practitioners match their observations to iris charts which divide the iris into zones corresponding to specific parts of the human body [5].

Liljequist et al. [6] have noticed irises changes that correlate to different illnesses. They depicted in their publications very similar iris charts based on their own observations. Lane [7] carried out further surgical and autopsy correlations with iris markings which sparked the effort of Jensen [5] develops an updated iris charts that are widely used among iridologists as shown in Fig. 1. Typical charts divide the iris into approximately 80–90 zones. For example, the zone corresponding to the kidney is in the lower part of the iris, just beside 6 o'clock.

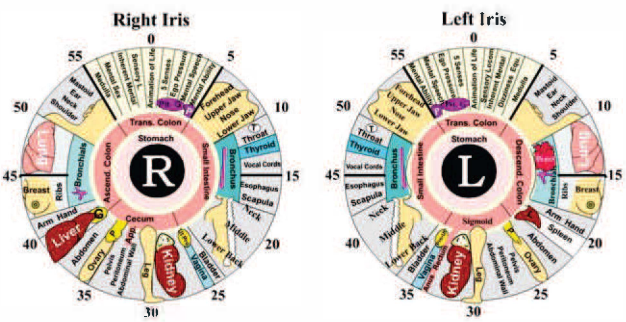

Fig 1. The iridology chart for both the right and left irises.

However, there are minor variations between charts' associations of body parts and areas of the iris. In an attempt

to evaluate the diagnostic validity of iridology, many investigations have been conducted without a control group, and some (with or without a control group) were not evaluator blinded. All of the uncontrolled studies and several of the un-blinded experiments suggested that iridology was a valid diagnostic tool [8].

A number of researchers used blinded evaluations of the diagnostic validity of iridology. Simon et al. [9] studied patients suffering from kidney disease as defined by a creatinine level, and compared these to controls who were free of kidney disease. Photographs were taken of both irises of all 146 study participants, coded, and shown to 3 experienced iridologists and 3 ophthalmologists. The resulting frequency of false-positive and false-negative diagnoses was not significantly different from that expected by chance. Knipschild [10] conducted another investigator-masked case–control study. His 39 patients had inflamed gallbladder disease as confirmed by subsequent surgery. Patients with jaundice were excluded. Controls were matched for age and sex and had no signs or symptoms of gallbladder disease and shown to the iridologists.

Despite the lack of evidence for iridology, it is important to note that conventional medicine does not ignore the eyes as indicators of disease. There is a wide spectrum of systemic diseases that correlates with eye changes (the iris, the sclera, and the conjunctiva). For example, jaundice can indicate liver disease, dilated pupils can indicate brain malfunction, and even rings around the iris can indicate Wilson's disease (an abnormality of copper metabolism). Advanced kidney disease induces eye findings that signal the need for initiation or intensification of therapy. Conjunctival erythema, termed the red eyes of uremia, may be noted when high plasma phosphate levels induce corneal and conjunctival precipitation of calcium pyrophosphate. Metastatic calcification in the eyes may be associated with elevations of the serum concentration of calcium or calcium-phosphate product [11]. Profound uremia may rarely be complicated by transient cortical blindness; this is termed uremic amaurosis, which occurs in association with preserved pupillary contraction on light exposure and normal fundoscopic findings [12].

Iridology, if proven correct, motivates healthy behavior and disease prevention throughout all stages of life which agrees with the objectives of pervasive healthcare technologies to offer new opportunities beyond traditional disease treatment that may play a major role in prevention. As indicated by Varshney [13], it was discussed the variability of health indicators between individuals and the manner in which relevant health indicators are provided to the users in order to maximize their motivation to mitigate or prevent unhealthy behaviors.

In this study, we evaluate the validity of iridology as a diagnostic tool. The case study in this research used iridology to detect abnormalities of the kidneys (chronic renal failure). We developed an automated technique based on acquiesced image of the iris, pre-processing, normalization, segmentation, and geometrical feature matching in regions corresponding to the kidneys in the iridology chart using the principles of iridology. The diagnosis was based on those features and on the medical conditions of the patient.

The rest of this paper are organized as follows: Section II dedicates to describe the proposed method, experimental results are drawn in Section III, and finally this paper is concluded in Section IV.

II. Proposed Method

It has long been recognized that there is a lack of standardized procedures used in iridology and this research tries to overcome some of the problems that hindered the recognition of iridology as a probable medical technique for diagnosis. In iridology, we call the lacunae gaps or openings in the iris tissue that indicate an inherent weakness in the affected organ and can go forward even result in chronic or destructive. The lacunae can be divided into open and closed. The open lake as its name suggests is open at one end rather than a complete circle. When the lake is open indicates that the problem is not solved completely. In contrast, the closed lagoon is enclosed by a flange on all sides.

A. Finding Iris Circle and its Radii

Circular Hough Transform (CHT) based algorithm is utilized for finding circles in images [14]. This approach is used because of its robustness in the presence of noise, occlusion and varying illumination. The CHT is not a rigorously specified algorithm, rather there are a number of different approaches that can be taken in its implementation. However, by and large, there are three essential steps which are common to all.

Circular Hough Transform Algorithm

- *Accumulator Array Computation*: Foreground pixels of high gradient are designated as being candidate pixels and are allowed to cast 'votes' in the accumulator array.
- *Center Estimation*: The votes of candidate pixels belonging to an image circle tend to accumulate at the accumulator array bin corresponding to the circle's center. Therefore, the circle centers are estimated by detecting the peaks in the accumulator array.
- *Radius Estimation*: If the same accumulator array is used for more than one radius value, as is commonly done in CHT algorithms, radii of the detected circles have to be estimated as a separate step.

It is worth mentioning that Radii are explicitly estimated utilizing the estimated circle centers along with image information. The technique is based on computing radial histograms and Fig. 2 shows the iris localization stages.

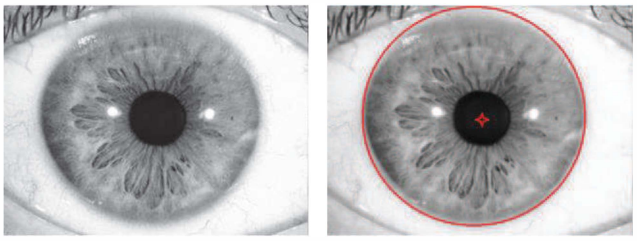

Fig 2. Stages of iris localization. Left, greyscale eye image. Right, a circle overlayed for iris and a star placed at the center of pupil.

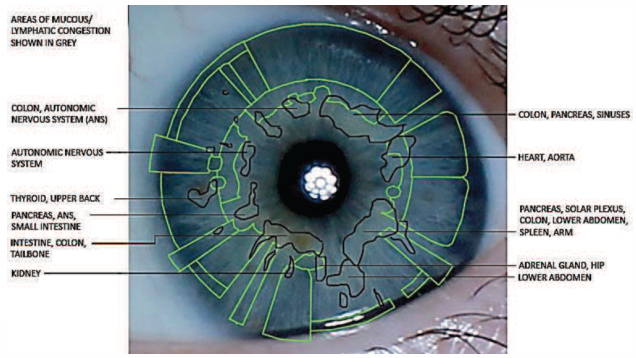

Fig 3. Mapping Iridology chart into extracted iris. Some notation are also provided in this image to show the possible abnormalities.

The CHT parameters are center coordinates (x_c, y_c) and the radius r, which are able to define any circle according to the equation (1).

$$x_c^2 + y_c^2 = r^2 \tag{1}$$

B. Mapping the Iridology Chart into Iris Image

Based on the Iridology map which is illustrated in Fig. 1, a flexible map is designed as an overarching layer for the iris image. An intuitive illustration of this geometrical map is shown in Fig. 3. In a technical view, this map is a specific segmentation which creates an Iridological partitioning so as to help the inference section to reach an accurate justification about the subject's abnormalities.

C. Geometrical Feature Extraction and Diagnosis

Hessian analysis was adopted to enhance several geometrical structures, including tube-like, blob-like, and plate-like structures [15], [16]. The principle of this analysis is to compute the second derivatives along the three dimensional directions by convoluting the iris image with derivatives of the Gaussian kernel. The Hessian matrix is defined by the following formula:

$$H_\sigma(x, y, z) = \begin{pmatrix} I_{xx} & I_{xy} & I_{xz} \\ I_{yx} & I_{yy} & I_{yz} \\ I_{zx} & I_{zy} & I_{zz} \end{pmatrix} \tag{2}$$

where the scale σ indicates the standard deviation of the Gaussian distribution and I_{ij} indicates the second deviation along the direction i-th and j-th. The scale σ could be used to control the radius of the enhanced blob-like structures. Large blob-like structures are enhanced when a high-scale value is used. The eigenvectors and eigenvalues ($|\lambda_1| \leq |\lambda_2| \leq |\lambda_3|$) can be computed by solving the Hessian matrix at each pixel.

The computed eigenvectors indicate three orthogonal directions of the detected object, and the eigenvalues indicate the degrees of curvatures along the corresponding directions. To enhance dark blob-like structures in the iris images, the likelihood of blob-like structures and the magnitude of the eigenvalues of a pixel can be formulated as follows:

$$R_B = \frac{|\lambda_1|}{\sqrt{|\lambda_2|\,|\lambda_3|}} \tag{3}$$

$$M = \sqrt{\lambda_1^2 + \lambda_2^2 + \lambda_3^2}$$

where R_B represents the likelihood of the blob-like structure and M represents the magnitude of the eigenvalues of a pixel. In the blob-like structures, the curvatures along three orthogonal directions should be high and similar. Therefore, R_B can achieve its maximum when the object is similar to the blob-like structure. In general, the magnitudes of the eigenvalues of objects are usually larger than the magnitude of the background. Therefore, M can be used to distinguish between the objects and the background. The blob-like structures can be enhanced using the equation 4.

$$B_\sigma(\boldsymbol{\lambda_p}) = \begin{cases} (1 - e^{-\frac{R_B}{2\alpha^2}})^2, & if\ \lambda_1 > 0, \lambda_2 > 0, \lambda_3 > 0 \\ 0, & otherwise \end{cases} \tag{4}$$

where $\boldsymbol{\lambda_p}$ indicates the eigenvalues at the position $p = (x, y, z)$ and α represents the sensitivity parameters of the terms R_B and M, respectively. The sensitivity parameter can control the weight of the corresponding term. In our study, the sensitivity parameter α was set to 0.5. This condition ($\lambda_1 > 0, \lambda_2 > 0$, and $\lambda_3 > 0$) only enhances dark objects. Because spots usually have different sizes, one single scale cannot detect all spots. To detect spots with different sizes, multi-scale blobness measurements can be used. The formula is as follows:

$$Blobness(\boldsymbol{\lambda_p}) = \max_{\sigma_{min} \leq \sigma \leq \sigma_{max}} B_\sigma(\boldsymbol{\lambda_p}) \tag{5}$$

where σ_{min} and σ_{max} are the minimum and the maximum scales, respectively. In iris images, small-scale blob detection segmented finer spot boundaries better compared to large-scale detection, where the spots were segmented into several fragmented regions. Large-scale blob detection could segment the main part of a spot with high internal echo, but the segmented result was coarser than that of small scale blob detection. In our experiments, multi-scale blob detection was performed with scales from 0.2 mm to 1.2 mm. The result after applying the multi-scale blobness measurement is shown in Fig. 4. Finally, connected component labeling [17] was adopted to group the enhanced pixels into candidate regions.

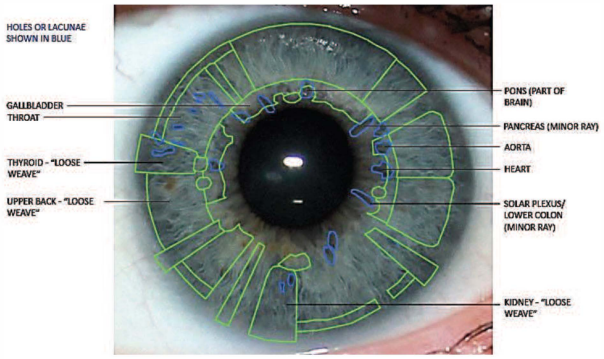

(a)

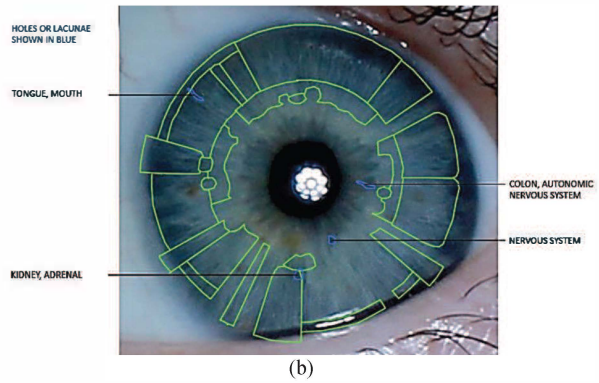

(b)

Fig 4. The result after applying the multi-scale blobness measurement into (a) Before treatment, and (b) after treatment iris images. Holes, deeper black areas, also called lacunae by iridologists.

III. Experimental Results

A database of iris images was constructed from CASIA Iris Image Database representing two images for each iris for both chronic renal failure group and healthy kidney group which add up to 680 pairs of images for both right and left iris. Every two pairs of subject's images are kept together and randomly arranged in their corresponding group of subjects. Those images are transformed to gray levels based on luminosity. The database images undertook another stage of transformation to be segmented and mapped to polar coordinates with a fixed size of 80 × 720 pixels for each image. The zones that corresponds to the kidney on the iris maps were then selected from the data base to be of size 40 × 24 pixels from point (40, 549) to point (80, 573) for the right iris and from point (40, 507) to point (80, 531) for the left iris.

The results in Table I for the testing subjects (56 subjects with chronic renal failure and 60 subjects with healthy kidney) show a correct diagnosis for both subjects with kidney problems and normal subjects of 82% and 93% in comparison with that of an experts does, respectively. While false diagnosis for the both groups are 6% and 2%, respectively. On the other hand, no diagnosis for subjects with kidney problems and normal subjects are 12% and 5%, respectively.

TABLE I. RESULT OF DIAGNOSIS IN COMPARISON WITH THAT OF AN EXPERTS DOES.

	Abnormal	Normal
Test Number	56	60
Correct Diagnosis	46	56
Miss Diagnosis	3	1
No Diagnosis	7	3

IV. Conclusion

In this paper, a method consists of (i) finding the center of iris and its radii, (ii) mapping iridology chart into extracted iris image, and (iii) geometrical analyzing characteristics of the iris were examined to find out abnormities in the iris zones of patient that correspond to the kidneys as claimed by the iridologists to classify the kidneys pathological conditions. The technique adopted in this research provides automated methods with artificial intelligence techniques to assess the correlation between the iris and the kidneys health. The diagnosis technique used shares similarities to that used in the iris biometric identification technique which uses the unique epigenetic patterns of a human iris for personal identification. Biometric identification employs image processing and signal processing methods to extract information from the unique iris structure from a digitized image of an eye though coding the wavelet coefficients for the main iris texture. While the technique used here identifies the fine discrepancies that appear in the iris texture through a fast blob detection and localization method.

References

[1] M.M. Dehshibi, A. Bastanfard, A new algorithm for age recognition from facial images, Publisher, City, 2010.
[2] M.M. Dehshibi, M. Fazlali, J. Shanbehzadeh, Linear principal transformation: toward locating features in N-dimensional image space, Publisher, City, 2014.
[3] M.M. Dehshibi, R. Allahverdi, Persian Vehicle License Plate Recognition Using Multiclass Adaboost, Publisher, City, 2012.
[4] M. Ramin, P. Ahmadvand, A. Sepas-Moghaddam, M.M. Dehshibi, Counting the Number of Cells in Immunocytochemical Images Using Genetic Algorithm, in: Hybrid Intelligent Systems (HIS), 2012 12th International Conference on, IEEE, 2012, pp. 185-190.
[5] B. Jensen, Iridology simplified, Book Publishing Company, 2012.
[6] N. Liljequist, The Diagnosis from the Eye, in, The Iridology Publishing Co, 1916.
[7] H.E. Lahn, Iridology: The Diagnosis from the Eye, 1914, Kessinger Publishing, 2003.
[8] K. Münstedt, S. El-Safadi, F. Brück, M. Zygmunt, A. Hackethal, H.-R. Tinneberg, Can iridology detect susceptibility to cancer? A prospective case-controlled study, Publisher, City, 2005.
[9] A. Simon, D.M. Worthen, J.A. Mitas, An evaluation of iridology, Publisher, City, 1979.
[10] P. Knipschild, Looking for gall bladder disease in the patient's iris, Publisher, City, 1988.
[11] C.-H. Hsiao, A. Chao, S.-Y. Chu, K.-K. Lin, L. Yeung, D.-T. Lin-Tan, J.-L. Lin, Association of severity of conjunctival and corneal calcification with all-cause 1-year mortality in maintenance haemodialysis patients, Publisher, City, 2011.
[12] H.R. Tyler, Neurologic disorders seen in the uremic patient, Publisher, City, 1970.
[13] U. Varshney, Pervasive healthcare, Publisher, City, 2003.
[14] S.J.K. Pedersen, Circular hough transform, Publisher, City, 2007.
[15] A.F. Frangi, W.J. Niessen, K.L. Vincken, M.A. Viergever, Multiscale vessel enhancement filtering, in: Medical Image Computing and Computer-Assisted Interventation—MICCAI'98, Springer, 1998, pp. 130-137.
[16] Y. Sato, S. Nakajima, N. Shiraga, H. Atsumi, S. Yoshida, T. Koller, G. Gerig, R. Kikinis, Three-dimensional multi-scale line filter for segmentation and visualization of curvilinear structures in medical images, Publisher, City, 1998.
[17] M.B. Dillencourt, H. Samet, M. Tamminen, A general approach to connected-component labeling for arbitrary image representations, Publisher, City, 1992.